THRESHOLD STRESS INTENSITY FACTOR FOR HYDROGEN-ASSISTED CRACKING OF CR-MO STEEL USED AS STATIONARY STORAGE BUFFER OF A HYDROGEN REFUELING STATION

Matsumoto, T.[1], Kubota, M.[2], Matsuoka, S.[2, 3], Ginet, P.[1], Furtado, J.[4] and Barbier, F.[4]
[1] K. K. AIR LIQUIDE LABORATORIES, 28 Wadai, Tsukuba, Ibaraki, 300-4247, Japan
[2] International Institute for Carbon-Neutral Energy Research (WPI-I^{2}CNER), Kyushu University, 744 Motooka, Nishi-ku, Fukuoka, 819-0395, Japan
[3] Research Center of Hydrogen Industrial Use and Storage (HYDROGENIUS), 744 Motooka, Nishi-ku, Fukuoka, 819-0395, Japan
[4] Air Liquide R&D, Paris-Saclay Research Center, 1 chemin de la Porte des Loges BP 126, Les Loges-en-Josas, 78354 – Jouy-en-Josas cedex, France
Corresponding author email: takuya.matsumoto@airliquide.com

ABSTRACT

In order to determine appropriate value for threshold stress intensity factor for hydrogen-assisted cracking (K_{IH}), constant-displacement and rising-load tests were conducted in high-pressure hydrogen gas for JIS-SCM435 low alloy steel (Cr-Mo steel) used as stationary storage buffer of a hydrogen refuelling station with 0.2 % proof strength and ultimate tensile strength equal to 772 MPa and 948 MPa respectively. Thresholds for crack arrest under constant displacement and for crack initiation under rising load were identified. The crack arrest threshold under constant displacement was 44.3 MPa·m$^{1/2}$ to 44.5 MPa·m$^{1/2}$ when small-scale yielding and plane-strain criteria were satisfied and the crack initiation threshold under rising load was 33.1 MPa·m$^{1/2}$ to 41.1 MPa·m$^{1/2}$ in 115 MPa hydrogen gas. The crack arrest threshold was roughly equivalent to the crack initiation threshold although the crack initiation threshold showed slightly more conservative values. It was considered that both test methods could be suitable to determine appropriate value for K_{IH} for this material.

1. INTRODUCTION

To ensure the safety of steel storage buffers of hydrogen refuelling station, a leak-before-break (LBB) assessment shall be performed in accordance with ASME BPVC 2013 Sec. VIII – Div. 3 Article KD-10 [1]. Threshold stress intensity factor for hydrogen-assisted cracking (K_{IH}) is used for the assessment and the K_{IH} can be obtained from constant displacement test or rising load test. However, there is still a matter of discussion which test method is more suitable for determining K_{IH}. Nibur *et al*. [2] performed rising-displacement and constant displacement tests in accordance with ASTM E1820-09 [3] and ASTM E1681-03 [4] in 103 MPa hydrogen gas using Cr-Mo and Ni-Cr-Mo low alloy steels with several strengths and reported that the threshold stress intensity factors were not equivalent, *i.e*. the discrepancies were 34 MPa·m$^{1/2}$ to 57 MPa·m$^{1/2}$ when the yield strengths were less than 783 MPa. Wada [5] conducted rising-load and constant-displacement test in 85 – 90 MPa hydrogen gas using a Ni-Cr-Mo low alloy steel with ultimate tensile strength equal to 942 MPa and reported that the crack initiation threshold under rising load was 46 MPa·m$^{1/2}$ while the estimated crack arrest threshold under constant displacement was more than 60 MPa·m$^{1/2}$. As described above, the value of K_{IH} strongly depends on the standards and the test methods. The aim of this study is to clarify what is the most suitable test method in order to determine the value of K_{IH} appropriate for the LBB assessment.

2. EXPERIMENTAL PROCEDURES

2.1 Material

A low alloy steel of JIS-SCM435 (Cr-Mo steel) used as real stationary storage buffer of a hydrogen refuelling station was examined in this study. The storage buffer had a nominal outer diameter of 355.6 mm and nominal wall thickness of 40.5 mm. The material of storage buffer was quenched and tempered. Tensile test specimens with the diameter of parallel portion equal to 5 mm were fabricated from the mid-thickness position of the wall along the longitudinal direction, and then

tensile tests were conducted in air at room temperature. The 0.2 % proof strength ($\sigma_{0.2}$) and the ultimate tensile strength (σ_{UTS}) were 772 MPa and 948 MPa respectively. The plane strain fracture toughness (K_{IC}) obtained in accordance with JSME S001-1992 [6] using CT specimens which were sampled from the buffer along *C-L* orientation with the sizes of 50.8 mm in width (W) and 12.7 in thickness (B) was 116 MPa·m$^{1/2}$ in air at room temperature.

2.2 Constant displacement test

Wedge-opening-load (WOL) specimens for constant displacement tests were designed according to ASTM E1681-03 [4] with dimensions shown in Figure 1. The WOL specimens were oriented so that the loading and crack growth directions were parallel to the circumferential and longitudinal axes, respectively, of the storage buffer (*C-L* orientation). Side-grooves were machined along the faces of the WOL specimens prior to pre-cracking, which reduced the specimen thickness by 15 %. Fatigue pre-cracking was introduced in air at test frequencies (f) of 10 Hz and 20 Hz with a stress ratio (R) of 0.1. The pre-crack length (a) was 0.5W. Maximum stress intensity factor during pre-cracking ($K_{pre\text{-}crack}$) was 15 MPa·m$^{1/2}$. Strain gauges were attached on the back face of the WOL specimens as shown in Figure 2, in order to measure loads caused by tightening bolts and to monitor crack growth during high-pressure hydrogen gas exposure. After the fatigue pre-cracking, the WOL specimens were statically loaded by a fatigue testing machine in order to calibrate the relationship between load (P) and back face strain (BFS) for the final crack length. Referring to the relationship, the loading bolt was tightened in air until the stress intensity factors reached the given values. The following equations [7] were used for the calculation of stress intensity factor (K). To consider the specimen thickness at the side-groove root (B_N), B in the reference [7] was replaced by $(BB_N)^{1/2}$.

$$K = (P/(BB_N W)^{1/2} \cdot f_I(a/W)) \quad , \tag{1}$$

$$f_I(a/W) = (2 + a/W)(0.8072 + 8.858(a/W) - 30.23(a/W)^2 + 41.088(a/W)^3 - 24.15(a/W)^4 + 4.951(a/W)^5)/(1 - a/W)^{3/2} \quad , \tag{2}$$

The bolt-loaded WOL specimens were placed into a stainless steel pressure vessel, and then exposed to 35 MPa or 115 MPa hydrogen gas for 1000 h at room temperature. After the exposure, the variations of BFS during unloading by loosening bolts were measured, then the WOL specimens were statically re-loaded by a fatigue testing machine to determine the final load (P_{fin}). Subsequently, the WOL specimens were fractured by fatigue test and the final crack lengths (a_{fin}) were measured from the fracture surfaces. Crack arrest threshold stress intensity factors were calculated with Eq. (1) and (2) using P_{fin} and a_{fin}.

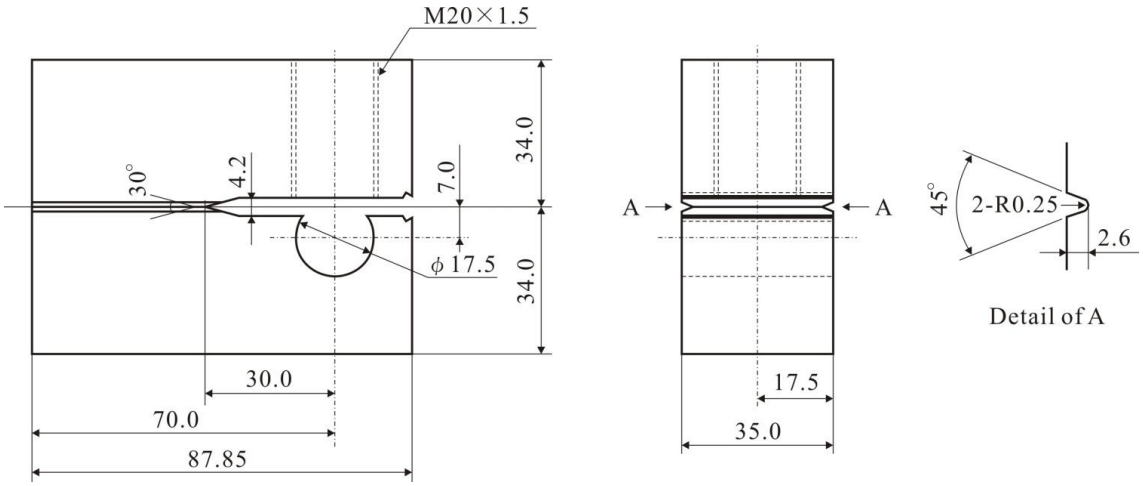

Figure 1. Shape and dimensions of WOL specimen (mm)

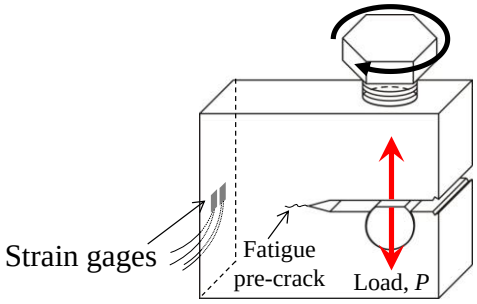

Figure 2. Attachment of strain gauges on back face of WOL specimen

2.3 Rising load test

Compact-tension (CT) specimens were fabricated for rising load tests with dimensions shown in Figure 3. The orientation of the CT specimens relative to the storage buffer was the same as the WOL specimens, *i.e.*, *C-L* orientation. Side-grooves were machined along the side faces of the specimens in the same plane as the pre-crack starter notch, which reduced the specimen thickness in this plane by 15 %. Fatigue pre-crack was introduced in air at room temperature at f of 20 Hz with a R of 0.1to a of 0.5W under $K_{\text{pre-crack}}$ of 10 and 27.7 MPa·m$^{1/2}$. The reason why $K_{\text{pre-crack}}$ has such wide range was that the crack initiation thresholds under rising load were found to be close to the $K_{\text{pre-crack}}$ of 27.7 MPa·m$^{1/2}$. Therefore, $K_{\text{pre-crack}}$ was decreased to 10 MPa·m$^{1/2}$ for some specimens. After the fatigue pre-cracking, two types of rising load tests, which were stepwise rising load test and monotonic rising load test, were conducted in high-pressure hydrogen gas at room temperature.

Stepwise rising load tests were performed in accordance with ISO 11114-4 method B [8]. Firstly, the CT specimens were monotonically loaded in 115 MPa hydrogen gas under displacement control at a displacement rate (V) equal to 2 × 10^{-3} mm/s. After the load reached the target load, the specimen was held at a constant displacement for 20 min, then the stress intensity factor was increased by an increment of 1 MPa·m$^{1/2}$. This procedure was repeated until crack initiation. The crack initiation threshold was defined as the value where the load decreased during the holding as shown in Figure 4 (a).

The procedure of monotonic rising load tests was similar to ASTM E399-09 [9]. Namely, the specimens were monotonically loaded without stepwise loading until crack initiations occurred. The crack initiation threshold was defined as the value when the load decreased as shown in Figure 4 (b). Because the displacement rate should be slow enough to detect the crack initiation, displacement rate was 2 × 10^{-5} mm/s.

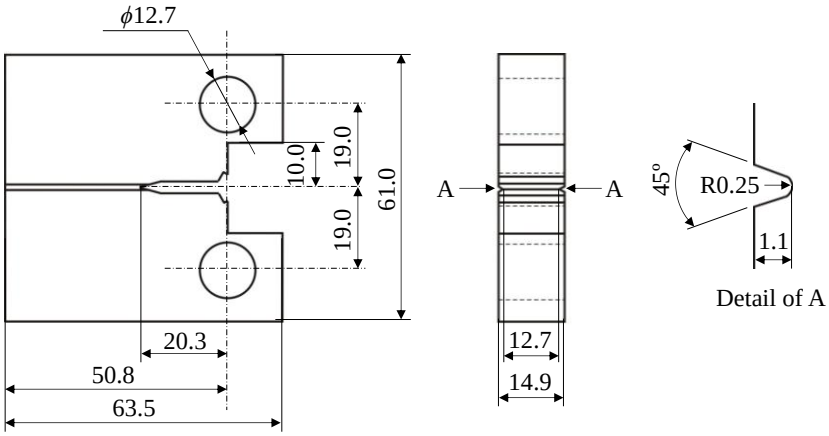

Figure 3. Shape and dimensions of CT specimen

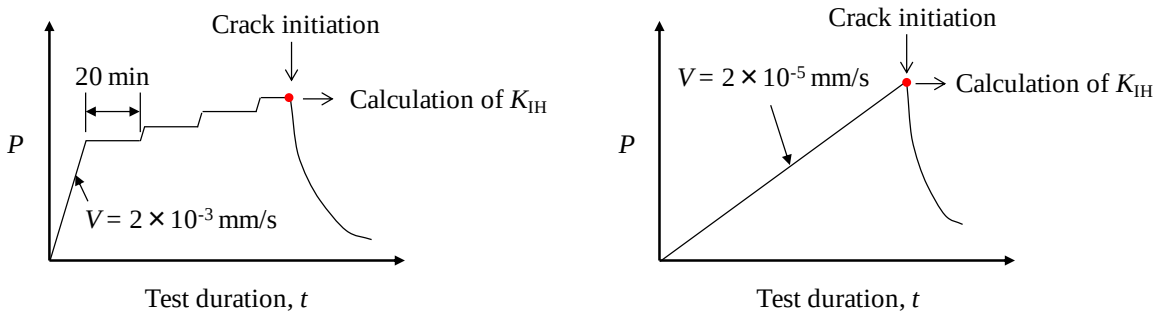

(a) Stepwise rinsing load test (b) Monotonic rising load test

Figure 4. Schematic diagrams of rising load tests

3. RESULTS AND DISCUSSION

3.1 Microstructures and Vickers hardness

Figure 5 shows the optical microscope images of the microstructure of the surface normal to the longitudinal direction of the storage buffer. The specimen was etched with 3 % nital. Since the storage buffer was quenched and tempered, it was considered that the microstructure was bainite or tempered martensite. However, the observation of microstructure revealed grains with white appearance (W microstructure) and grains with black appearance (B microstructure) as shown in Figure 5 (a) and (b). It was considered that the heterogeneous microstructure was formed due to the difficulty of heat treatment because the storage buffer had large wall thickness (= 40.5 mm).

In order to investigate the microscopic hardness, Vickers hardness testing was performed for each microstructure. The measurement load was 0.01 kgf and the holding time was 30 s. Figure 6 shows the results of the Vickers hardness tests. The average hardness of the W microstructure and the B microstructure were HV270 and HV331 respectively. Although the detail mechanism which caused such difference had not been clarified, it was presumed that the B microstructure was more susceptible to hydrogen embrittlement because the hardness of the B microstructure was higher than that of the W microstructure.

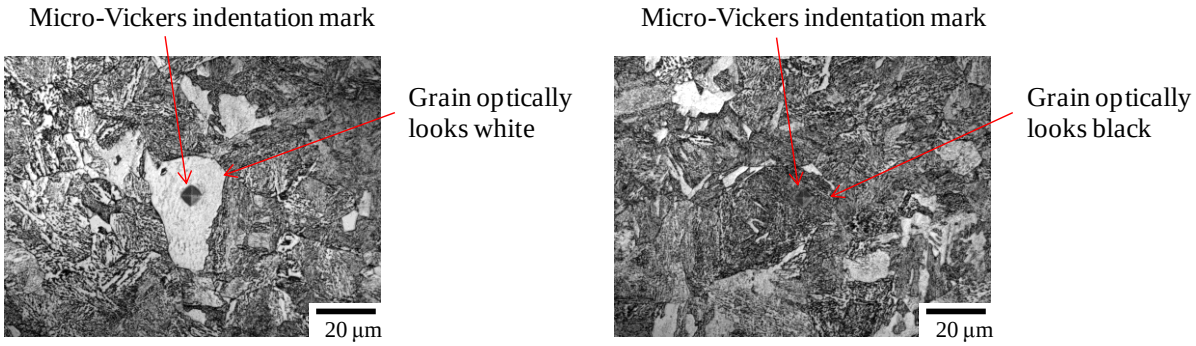

(a) Microstructure optically looks white (b) Microstructure optically looks black

Figure 5. Optical images of microstructures

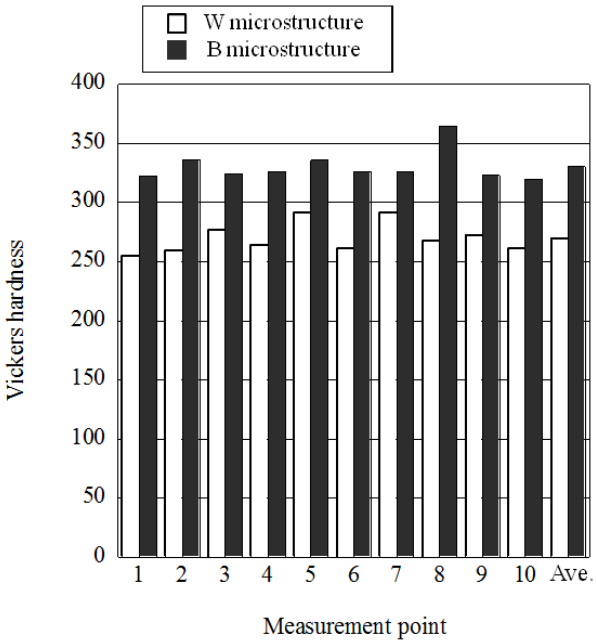

Figure 6. Micro-Vickers hardness of W microstructure and B microstructure

3.2 Crack arrest thresholds in high-pressure H_2 gas

Figure 7 shows the representative variation in *BFS* during 115 MPa hydrogen gas exposure. The symbol of K_{app} means the initial applied stress intensity factor by bolt-loading. The crack initiation and the crack arrest were clearly determined from the change in *BFS*. The fact that the stop of the crack propagation is confirmed is critically important to determine threshold values. Figure 8 shows plots of K_{app} *vs.* incubation time. Although the incubation time varied greatly even at the same K_{app}, the incubation time had a tendency to increase as K_{app} decreased. The crack initiation threshold for the constant displacement test was 65 MPa·m$^{1/2}$. This value met the following small-scale yielding (SSY) and plane-strain validity criteria required in ASTM E1681-03 [3].

$$B,\ a,\ a - W \geq 2.5\ (K/\sigma_{0.2})^2 \quad . \tag{3}$$

Figure 9 shows the relationship between crack arrest thresholds and K_{app}. The crack arrest thresholds which met Eq. (3) were 44.3 MPa·m$^{1/2}$ and 44.5 MPa·m$^{1/2}$. Some results which did not meet Eq. (3) were slightly higher than those values, but all the crack arrest thresholds were much smaller than the crack initiation threshold (= 65 MPa·m$^{1/2}$) under constant displacement test. According to ASTM E1681-03 [3], stress intensity factor threshold for plane strain environment-assisted cracking (K_{IEAC}) is defined as the highest value of the stress intensity factor at which crack growth is not observed. However, crack arrest threshold shall be used for LBB assessment especially in high-pressure hydrogen gas because the crack arrest thresholds were much smaller than K_{IEAC}. The constant displacement tests were also conducted in 35 MPa hydrogen gas. The crack arrest threshold, which met Eq. (3), was 53.2 MPa·m$^{1/2}$.

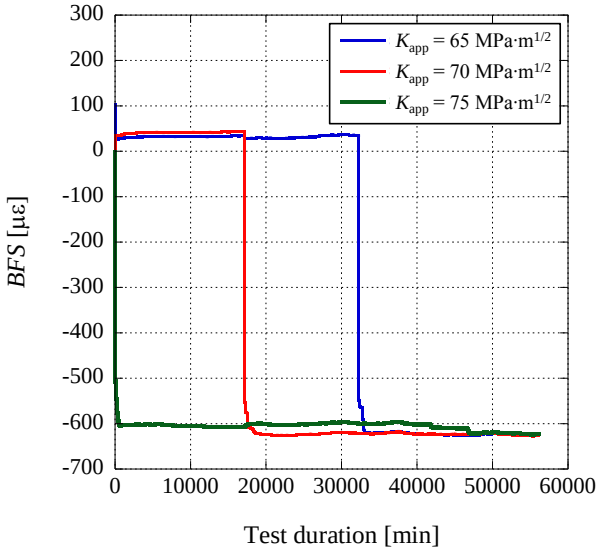

Figure 7. Variation in *BFS* during constant displacement tests during 115 MPa hydrogen exposure

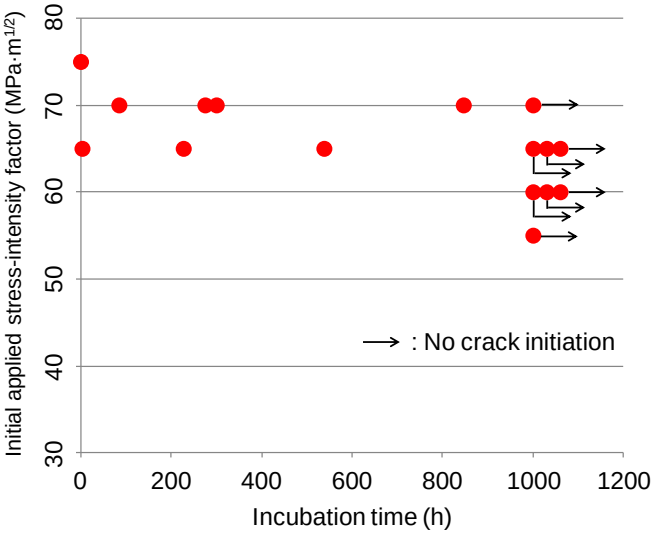

Figure 8. Plots of initial applied stress-intensity factor *vs.* incubation time

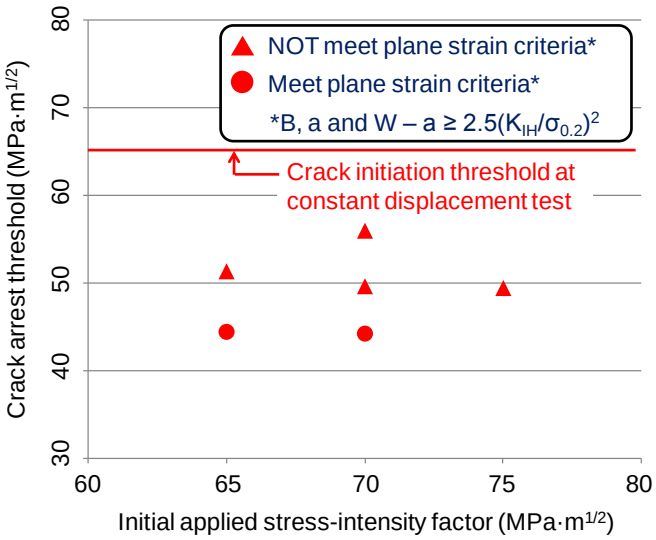

Figure 9. Crack arrest thresholds in 115 MPa hydrogen gas from constant displacement tests

3.3 Crack initiation thresholds in high-pressure H_2 gas

Figure 10 shows the typical example of relationship between load and time duration (*P-t* curve) for stepwise rising load tests in 115 MPa hydrogen gas at $K_{pre\text{-}crack}$ of 10 MPa·m$^{1/2}$. The load dropped at 11.6 kN and the crack initiation threshold was 35.9 MPa·m$^{1/2}$. When $K_{pre\text{-}crack}$ was 27.7 MPa·m$^{1/2}$, the crack initiation threshold was 33.1 MPa·m$^{1/2}$. According to ISO 11114-4 method B [8], $K_{pre\text{-}crack}$ shall be less than 60 % of crack initiation threshold (19.9 MPa·m$^{1/2}$ for this study) but there was no clear effect of $K_{pre\text{-}crack}$ in the range of 10.0 MPa·m$^{1/2}$ to 27.7 MPa·m$^{1/2}$ on the crack initiation thresholds.

Figure 11 shows the *P-t* curve for a monotonic rising load test in 115 MPa hydrogen gas at $K_{pre\text{-}crack}$ of 10 MPa·m$^{1/2}$. The load dropped at 11.4 kN and the crack initiation threshold was 35.3 MPa·m$^{1/2}$. The crack initiation threshold at $K_{pre\text{-}crack}$ of 27.7 MPa·m$^{1/2}$ was 41.1 MPa·m$^{1/2}$. In terms of the crack initiation thresholds, there were little difference between the stepwise rising load tests and the monotonic rising load tests. A monotonic rising load test was also performed in 35 MPa hydrogen gas. The crack initiation threshold was 52.4 MPa·m$^{1/2}$. All the crack initiation thresholds satisfied Eq. (3).

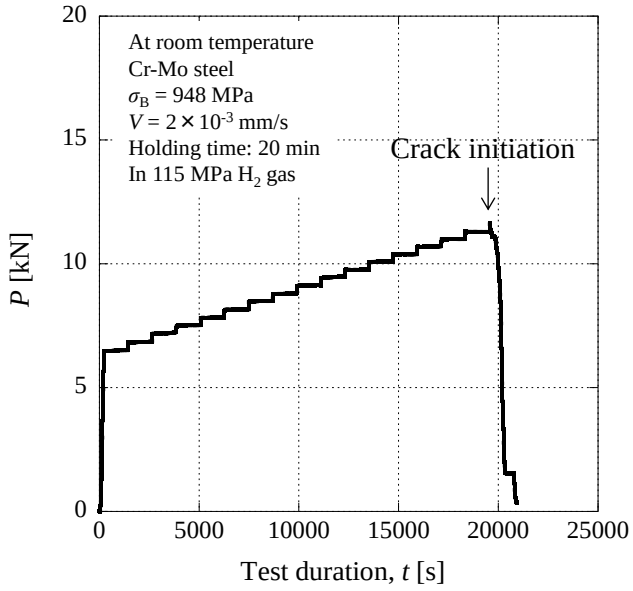

Figure 10. Relationship between load and test duration for stepwise rising load test in 115 MPa hydrogen gas ($K_{pre\text{-}crack}$ = 10 MPa·m$^{1/2}$ at fatigue pre-cracking)

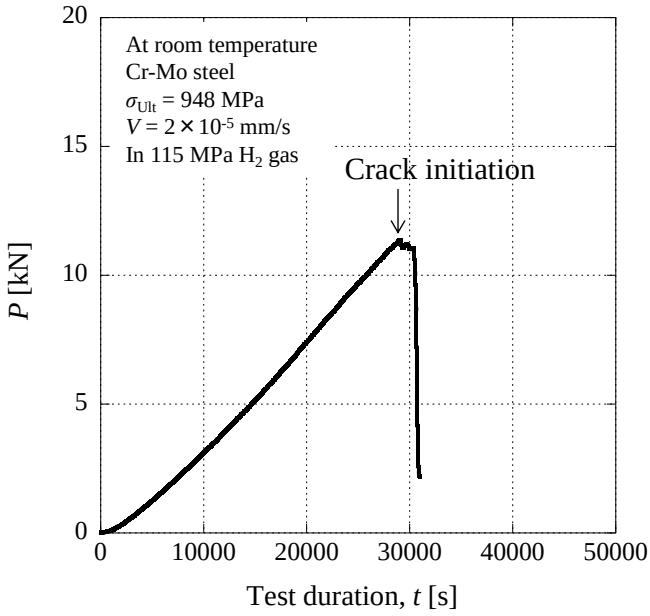

Figure 11. Relationship between load and test duration for monotonic rising load test in 115 MPa hydrogen gas ($K_{pre\text{-}crack}$ = 10 MPa·m$^{1/2}$ at fatigue pre-cracking)

3.4 Comparison between crack arrest thresholds and crack initiation thresholds

Table 1 summarizes the results from the constant displacement tests and the rising load tests. Figure 12 shows the comparison of the crack arrest thresholds and the crack initiation thresholds. The crack arrest thresholds from the constant displacement tests were roughly coincident with the crack initiation thresholds from the rising load tests in 35 MPa and 115 MPa hydrogen gas although the crack arrest thresholds were slightly higher than the crack initiation thresholds in 115 MPa

hydrogen gas. Wada *et al*. [10] conducted rising load tests and constant displacement tests in 45 MPa hydrogen gas using a similar kind of Cr-Mo steel (JIS-SCM435) having 781 MPa of $\sigma_{0.2}$ and 958 MPa of σ_{UTS}. According to their study, the crack initiation threshold from the rising load test was 44 MPa·m$^{1/2}$ and no crack extension were observed at the maximum K_{app} equal to 55 MPa·m$^{1/2}$ in the constant displacement tests. These results were coincident with the result in this study. Therefore, it was considered that both test methods in this study were suitable to determine appropriate value for K_{IH}.

On the other hand, Nibur *et al*. [2] reported that there was big difference between the crack initiation thresholds and the crack arrest thresholds in 103 MPa hydrogen gas using SA372 grade *J* low alloy steel with $\sigma_{0.2}$ and σ_{UTS} equal to 783 MPa and 907 MPa respectively. They reported that the crack-initiation and crack-arrest thresholds were 47 MPa·m$^{1/2}$ and 81 MPa·m$^{1/2}$ respectively. The crack initiation threshold was relatively close to our results but the crack arrest threshold was much higher than our results. Regarding the causes of the difference, three reasons could be considered. First one is the effect of specimen sizes, *i.e*., SSY and plane-strain criteria in Eq. (3). In this study, the crack arrest thresholds which satisfied Eq. (3) were used to compare with the crack initiation thresholds but Nibur *et al*. used smaller WOL specimens with *W* and *B* equal to 56.9 mm and 22.2 mm respectively, which did not satisfy Eq. (3). Since it is known that specimen sizes strongly affect fracture toughness, the cause of the difference could be due to specimen sizes although Nibur et al. confirmed from FEM analysis and experiments that the crack arrest threshold was not dependent on *a/W*. Second one is due to different test method for each rising load test. Nibur *et al*. conducted the rising displacement tests in accordance with ASTM E1820-09 [3] while ISO 11114-4 method B [8] and ASTM E399-09 [9] were applied except loading rate in this study. In ASTM E1820-09 [3], K_{IC} is calculated from J_{IC}, which is obtained from crack growth resistance curve (R-curve). Although R-curve method is generally used to determine K_{IC}, it's still under discussion whether the R-curve method shows the same results as ISO 11114-4 method B [8] and ASTM E399-09 [9] under hydrogen environment. Final one is due to the heterogeneous microstructure shown in Figure 5. In this study, the values of $\sigma_{0.2}$ and σ_{UTS} were 772 MPa and 948 MPa respectively, but the microscopic hardness varied with the inhomogeneous microstructures as shown in Figure 6, *i.e*., the Vickers hardness of W microstructure and B microstructure were HV270 and HV331 respectively. Kondo *et al*. [11] conducted crack propagation tests under continuous hydrogen charging using SCM440H low alloy steel and reported that the steel became markedly susceptible to hydrogen-assisted cracking when HV > 280. Therefore, it was considered that the B microstructure is more susceptible to hydrogen-assisted cracking. In other words, it was possible that the crack propagation selectively occurred in the B microstructure. According to the study by Nibur *et al*., the crack-arrest and the crack-initiation thresholds were 37 MPa·m$^{1/2}$ and 26 MPa·m$^{1/2}$ when $\sigma_{0.2}$ and σ_{UTS} were 900 MPa and 1001 MPa. In this study, if the crack propagation selectively occurred in the B microstructure, the material can be considered as a higher strength material and the results are consistent with the study by Nibur *et al*..

Table 1. Results from constant-displacement and rising-load tests.

	Constant displacement			Rising force		
H_2 pressure (MPa)	K_{app} (MPa·m$^{1/2}$)	K_{IH} (MPa·m$^{1/2}$)	SSY and plane-strain criteria	Loading method	K_{IH} (MPa·m$^{1/2}$)	SSY and plane-strain criteria
115	65	44.5	Valid	Stepwise	35.9	Valid
	65	51.4	Invalid		33.1	Valid
	70	49.7	Invalid	Monotonic	35.3	Valid
	70	44.3	Valid		41.1	Valid
	70	56.0	Invalid			
	75	49.5	Invalid			
35	75	53.2	Valid	Monotonic	52.4	Valid

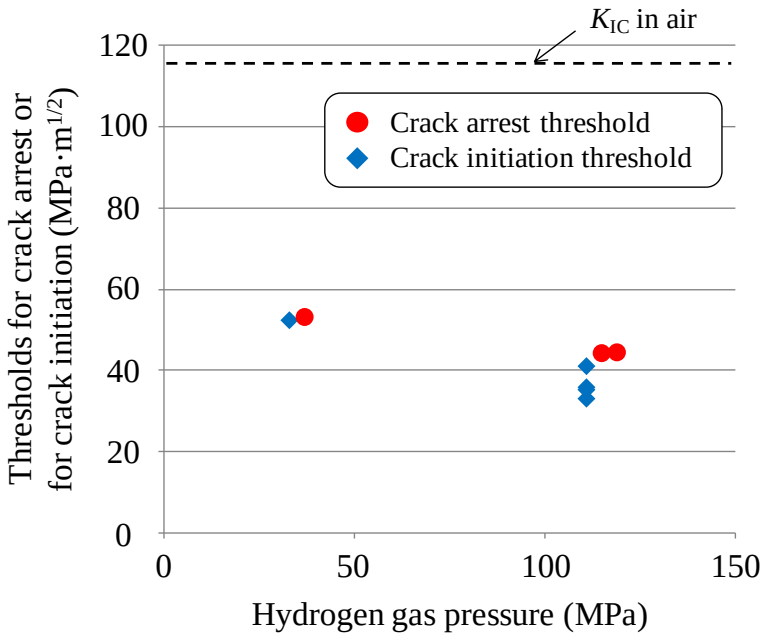

Figure 12. Comparison of crack-arrest and crack-initiation thresholds

4. CONCLUSIONS

Threshold stress intensity factor for hydrogen-assisted cracking, K_{IH}, of JIS-SCM435 low alloy steel (Cr-Mo steel) used as stationary storage buffer of a hydrogen refuelling station has been examined from constant-displacement and rising load tests in 35 MPa and 115 MPa hydrogen. The obtained results are as follows:

(1) Crack growth monitoring technique using back face strain gauges was established to detect crack initiation and crack arrest under constant displacement test during high-pressure hydrogen gas exposure.

(2) The crack initiation thresholds in the constant displacement tests were much higher than the crack arrest thresholds. The crack arrest threshold shall be used to determine appropriate value for K_{IH} rather than the crack initiation threshold in the constant displacement test.

(3) The crack arrest thresholds from the constant displacement tests were roughly coincident with the crack initiation thresholds from the rising displacement tests as far as small-scale yielding and plane strain criteria were satisfied. Both test methods of the constant-displacement and the rising-load tests were suitable to determine appropriate value for K_{IH}.

5. REFERENCES

1. ASME Boiler and Pressure Vessel Code (BPVC), Sec. VIII, Div. 3, 2013, Article KD-10, Special Requirements for Vessels in Hydrogen Service.
2. Nibur, K.A., Somerday, B.P., Marchi, C.S., Foulk, J.A.,III, Dadfarnia, M. and Sofronis, P., The Relationship Between Crack-Tip Strain and Subcritical Cracking Thresholds for Steels in High-Pressure Hydrogen Gas, Metall. Mater. Trans. A, 248, 2013, pp. 248-268.
3. ASTM E1820-09, Standard Test Method for Measurement of Fracture Toughness, 2009, ASTM International, West Conshohocken, PA.

4. ASTM E1681-03, Standard Test Method for Determining Threshold Stress Intensity Factor for Environment-Assisted cracking of Metallic Materials, 2008, ASTM International, West Conshohocken, PA.
5. Wada, Y., On Material Selection and Safety Assessment for Steel Storage Buffers of Hydrogen Refuelling Station, *Journal of Hydrogen Energy Systems Society of Japan*, 35, No. 4, 2010, pp. 38-44.
6. JSME S001-1992, Test method for Elastic Plastic Fracture Toughness J_{IC}, 1992, The Japan Society of Mechanical Engineering.
7. Murakami, Y., editor-in-chief, Stress Intensity Factor Handbook, Vol. 1, 1987, Pergamon Press, pp. 24-26.
8. ISO Standard 11114-4, 2005, Part 4, Test methods for selecting metallic materials resistant to hydrogen embrittlement.
9. ASTM E399-09, Standard Test Method for Linear-Elastic Plane-Strain Fracture Toughness K_{IC} of Metallic Materials, 2009, ASTM International, West Conshohocken, PA.
10. Wada, Y., Ishigaki, R., Tanaka, Y., Iwadate, T. and Ohnishi, K., Evaluation of Metal Materials for Hydrogen Fuel Stations, Papers of the International Conference on Hydrogen Safety, 8-10 September 2005, Italy.
11. Kondo, Y., Kubota, M. and Shimada, K., Hydrogen Enhanced Crack Propagation of SCM440H Low Alloy Steel under Long-Term Varying Load, *Eng. Fract. Mech.*, 77, 2010, pp. 1963-1974.